Seventh International Conference on Control, Automation,
Robotics And Vision (ICARCV'02), Dec 2002, Singapore

Automated Measurement of Brain Dimensions

KASIA MICHALAK[4], JAMES DEVENISH[4], ROBERT LINGGARD[4], KRIS PARKER[4], IRINA EMELYANOVA[4], LESLEY CALA[1], YIANNI ATTIKIOUZEL[4], NEIL HICKS[3], PETER ROBBINS[2], FRANK MASTAGLIA[5]
kasia@arcme.com, devenish@arcme.com, bobling@arcme.com

[1]Australian Research Centre for Medical Engineering (ARCME), The University of Western Australia, 35 Stirling Hwy, Crawley, WA 6009
[2] The West Australian Centre for Pathology and Medical Research (PathCentre), Hospital Avenue, Nedlands, WA 6009
[3]Sir Charles Gairdner Hospital, Verdun St, Nedlands, WA 6009
[4]ARCME, Murdoch University, South Street, Murdoch, WA 6150
[5]Centre for Neuromuscular and Neurological Disorders, The University of Western Australia, 35 Stirling Hwy, Crawley, WA 6009

Abstract: — This paper describes a technique for automating the measurement of brain width and length at the level of the bi-parietal diameter, by processing an axial computed tomography (CT) brain scan image. The development of this algorithm derives from the wish to normalise patient data according to skull size and shape, for the purpose of comparing new patient data with that from past cases. This algorithm uses image processing techniques to find the inner edge of the cavity of the skull. The width and length of the brain are measured as inner dimensions of this bone periphery. The main challenges facing this work are the structural asymmetry of the brain and the angle of rotation commonly encountered when working with axial CT images. Both of these must be taken into account prior to measuring the brain width and length. The algorithm was designed and tested to operate on a database containing CT brain scans from 530 patients. The results indicate that the algorithm has a 90.56% success rate.

Key-Words: — **CT brain scans**, normalisation, brain dimensions, skull measurement, axis of symmetry.

1 Introduction

The main motivation for this research work comes from the wish to provide a diagnostic aid to radiologists in the interpretation of CT brain scans. It is desirable that the CT data from a new patient be comparable with that from past cases in order to take advantage of previously successful diagnoses. In such a comparison, it is important to compare like with like, and so the task of normalisation arises. In particular, the skull size and shape (which differ from case to case) need to be normalised, or at least quantified.

Our study has undertaken the task of automating the measurement of the width and length of the internal cavity of the skull in an axial CT scan. Two main challenges were faced in the development of a suitable algorithm. The first was an extrinsic factor – the angle of rotation of a given patient's head within the axial CT scan. In taking a brain CT scan, the radiographer aligns the patient's head in a standard way. The convention is for the patient to lie supine, head-first on the CT table. The head is positioned with the nose facing upwards and aligned so that a vertical laser light projected onto the side of the patient's head corresponds to the virtual line joining the corner of the eye with the external auditory meatus. Despite this convention, occasionally such an alignment cannot be maintained by the patient (who may be unconscious or otherwise incapable of holding their head in the required position), or it may be impractical (such as in the case where it may result in airway blockage). As a result, the head in the axial CT scan may be rotated to a greater or lesser degree. Such rotations have to be taken into account prior to the measurement of brain width and length. The second challenge faced by the work presented here is an intrinsic factor — the bilateral asymmetry of the brain. The aetiology of brain asymmetry may be normal or pathological. Whilst normal human brains exhibit an approximate symmetry with respect to the interhemispheric fissure, pathological brains, such as those demonstrating midline-displacement or mass effect, may exhibit marked asymmetry. This fact impacts directly on the determination of the aforementioned angle of rotation. Section 2.2 discusses how these difficulties are overcome.

In comparing measurements of width and length of different brains, it is necessary that the measurements be made at the same anatomical level. In a previous paper [1], we described a method of measuring brain height automatically from the lateral scout image (view showing skull from the side) in a patient's CT scan image set. The brain height was defined as the distance from the midpoint of the orbitomeatal plane (the plane formed by the orbitomeatal lines on either side of the head, also referred to as the skull base-plane) to the inner table (top inner edge) of the skull vault. The level chosen for this study is that part of the head usually used to measure external skull width — the 'bi-parietal diameter'. (That is, the level of the interthalamic connexus). It was validated that this level is at approximately 37% of the average individual's brain height. This level is convenient because at this position the brain surface is only slightly convex, and any errors in finding this level will cause minimum error in the measurements of width and length. A typical axial image at the level of the bi-parietal diameter is shown in Figure 1.

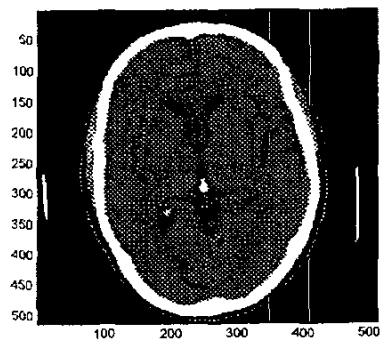

Fig. 1. A typical 512-by-512-pixel axial CT brain scan at the level of the bi-parietal diameter.

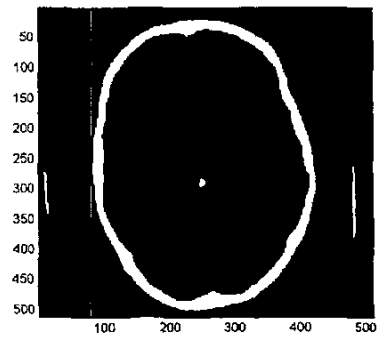

Fig. 2. The CT brain scan of Figure 1, thresholded at 200 H, clearly demarcates the skull from the surrounding tissue. The threshold also picks up some of the harder parts of the headrest, and an area of calcification within the skull.

2 Method

2.1 Edge Extraction

The first step in determining the width and length of a patient's brain at the bi-parietal diameter is to find the inner boundary of the skull in the axial image at this level. The inner bone boundary is used because it is a more easily identifiable "landmark" than the perimeter of the brain tissue itself. Furthermore, as the brain occupies the majority of the cranial volume, the inner skull boundary can be used as a proxy for our purposes.

The axial image is firstly binarised by applying an appropriate threshold. The measurement units used in CT scan images to represent X-ray attenuation are Hounsfield units (H) [2]. The skull (which provides the greatest attenuation and therefore appears white on the image) has Hounsfield values in the range 100-2000 H. A convenient threshold level is therefore 200 H. This ensures that everything from airways (with a Hounsfield range of −100-0 H) to skin (with a range of 0-80 H) will appear black on the thresholded image. Figure 2 illustrates the result of applying such a threshold to the image of Figure 1. The white fragment within the skull is a calcified normal structure, the pineal, and the linear fragments outside the skull are parts of the cross-section of the headrest on the CT table.

The next step is to extract the inner edge of the skull. This is achieved using an edge-following algorithm. If the edge follower is started inside the skull then the first edge it finds is the inner bone edge, which it then follows. The result of this process is a single-pixel-wide inner-skull boundary — a potentially closed outline depicting the shape of the inner boundary of the skull — hereafter referred to as the *shape boundary*. Applying our edge-follower to the image in Figure 2 yields the image shown in Figure 3.

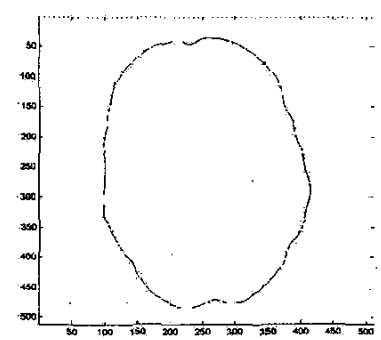

Fig. 3. A typical shape boundary: the result of applying an edge-following algorithm to the binary image of Figure 2.

2.2 Axis of Least Asymmetry

The measurement of brain (skull) width and length is not straightforward, because it is dependent on the orientation of the head in the CT brain scan image. In order to automate the measurement process, it is convenient to base the width and length measurements on the horizontal and vertical extents, respectively, of the shape boundary. Clearly, these extents differ depending on the orientation of the head, and therefore of the shape boundary, within the rectangular image frame. It was therefore necessary to define a standard orientation for the shape boundary, given that in the majority of CT brain scans encountered, the head was rotated. The standard orientation was chosen to be vertically "upright" in the image frame (with the nose facing "North"). This necessitates measuring the degree of rotation, if any, required to bring the axis of symmetry of a shape boundary into an "upright" position. Once upright, the width and length of a rectangle drawn to contain the shape boundary are taken to be the width and length of the brain itself.

In order to align the shape boundary in an upright position, it was decided to find its axis of symmetry, and to rotate the image so that this axis is vertical. Recall that a straight line is an axis of symmetry of a planar figure, if that figure is invariant to reflection with respect to that axis [3, 4]. The difficulty lies in the fact that the shape boundary is never perfectly symmetrical about any axis. A compromise is to determine instead the axis of *least asymmetry*, which for the sake of brevity we will hereafter refer to as the axis of symmetry.

If the axis of symmetry of the shape boundary is orientated at θ degrees from the vertical, then the shape boundary reflected about the axis of symmetry will be orientated at an angle of $-\theta$ degrees to the vertical. Note that both the shape boundary and its reflection share a common centroid. We presume that the maximum correlation between the original and reflected shape boundaries will occur when the shape boundary is rotated about the centroid by 2θ. Conversely, if the shape boundary is rotated by half of 2θ, it will be vertically upright.

The shape boundary can be represented as a *radius function*. That is, a set of radii taken from the centroid of area of the shape enclosed by the shape boundary, to the points on the boundary itself. For convenience, the radii are calculated at 1024 equally-spaced angles over 2π radians. The use of 1024 radial samples is sufficient to accurately model the shape boundary and also facilitates fast Fourier decomposition, as described in our companion paper [5]. It is worthwhile noting that angular measurements have been made according to a system wherein "North" is 0 radians, "East" is $\pi/2$ radians, "South" is π radians, and "West" is $3\pi/2$ radians. The first radial sample is made at the 0 radians, and the last at $(1023*2\pi)/1024$ radians. The radius function of the shape boundary shown in Figure 3 is illustrated in Figure 4. Note that if the shape boundary were perfectly symmetrical about the vertical axis, then its radius function would also be symmetrical. That is, the radius at angle θ would be the same as the radius at angle $(2\pi-\theta)$.

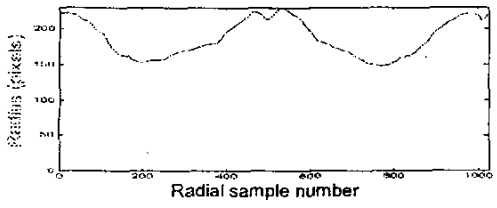

Fig. 4. The radius function of the skull boundary shown in Figure 3.

A translation in the radius function is equivalent to a rotation of the shape it represents. Hence, by finding the shift which gives maximum correlation between the radius function and its reverse, we not only find the axis of symmetry, but also the rotation necessary to align this axis with the vertical axis of the image. To expedite the correlation process we use the sum of squared errors, rather than true mathematical correlation, and find the shift that gives the minimum sum. In this manner, our work differs to that of Liu and co-workers [6, 7].

Figure 5 shows the radius function of the shape boundary together with its reverse. The sums of squared errors of these two functions, for shifts in the range -50 to $+50$ samples, are shown in Figure 6. Given that there are 1024 equally spaced radii, each radius is at an angle of $2\pi n/1024$ radians, with n being the sample index. Each shift is therefore equivalent to a rotation of the shape boundary by $2\pi/1024$ radians.

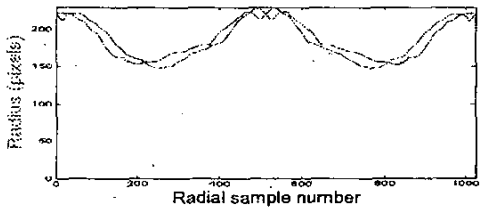

Fig. 5. The radius function and its reverse.

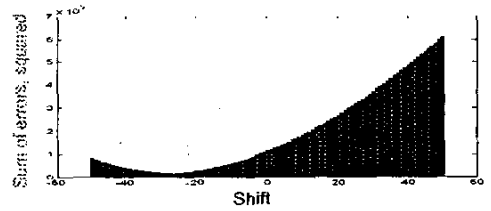

Fig. 6. Histogram depicting the sum of errors squared between the radius function and its reverse, for shifts of -50 to 50 samples. The minimum is at -28, which is equivalent to $-28*2\pi/1024$ radians, or -9.84 degrees.

The minimum value of the sum of squared difference between the radius function and its shifted reverse (and therefore the maximum correlation between the two) in the above example is at a shift of -28. This is equivalent to an angle of rotation of -9.84 degrees. If the shape boundary of Figure 3 is rotated by half this amount then its axis of symmetry will be aligned with the vertical axis of the image, as illustrated in Figure 7.

Finally, we enclose the vertically upright shape boundary within a rectangle, the width (W) of which is defined as brain width and the length (L) of which is defined as brain length. Figure 8 illustrates this situation. In this case, W=318 pixels and L=445 pixels. The spacing between pixels is approximately 0.42 mm and therefore the width and length of the brain are 132.5 mm and 184.4 mm, respectively.

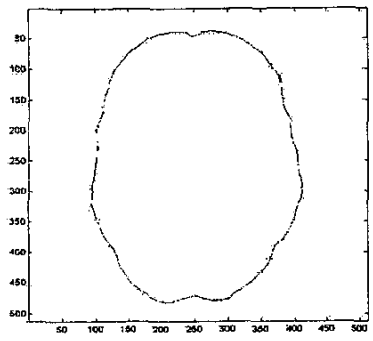

Fig. 7. The shape boundary, rotated –4.92 degrees about its centroid so that its axis of symmetry is vertical.

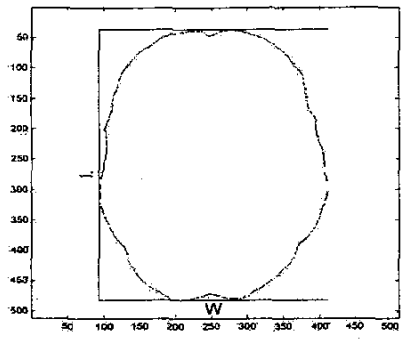

Fig. 8. The width and length of a rectangle drawn around the perimeter of the upright shape boundary are taken to be the width and length of the skull, and therefore the brain.

3 Results

The algorithm was tested on a database containing 530 patients — 279 females and 251 males — aged 14 to 98 years. The data was obtained from pre-existing studies provided by Sir Charles Gairdner Hospital. All scans were made on living patients with or without focal abnormalities. The images were obtained as 512×512 axial slices with varying thickness of 3-6mm. Use of the data was permitted by the Human Research Ethics Committee at Sir Charles Gairdner Hospital. Trial 2000-136 serves as the Licence number to the Principal Investigator Adjunct Professor Lesley Cala. All the data was acquired with a GE Medical Systems HiSpeed CT/i scanner. The algorithm was performed at the bi-parietal level on all cases, using the provided scout for localisation. The non-contrast series was used in all cases. In cases where a slice at the bi-parietal level was unavailable, a slice was synthesised using nearest-neighbour interpolation.

Of the 530 cases, 457 had correct results (correct rotation, resulting in visually correct width and length) after being individually checked by hand. Removing all the cases where incorrect rotation was a result of image acquisition (for example, where the pitch of the head was insufficiently accounted for by the gantry tilt, resulting in not truly bi-parietal slices) leaves 50 cases where the axis of symmetry (and hence, the angle of rotation) was found incorrectly. This represents a success rate of 90.56%.

4 Discussion

In developing the algorithm, it quickly became apparent that the edge-follower needs to cope with the situation when surgical burr holes are present, or pieces of the skull bone have been removed. To this end, the algorithm was modified to interpolate small (<50 pixel wide) gaps in the skull, using a simple median filter to determine the end-points prior to interpolation. For gaps larger than 50 pixels, the algorithm checks to see if a bone fragment exists in the gap (i.e. two burr holes are present). If a fragment does exist, the data is included, and the edge follower interpolates the gaps at each end of the fragment. Finally, if no fragment exists, it simply interpolates the gap. The results of applying the edge-follower to a skull with a large piece of bone removed, and one with two surgical burr holes, are shown in Figure 9.

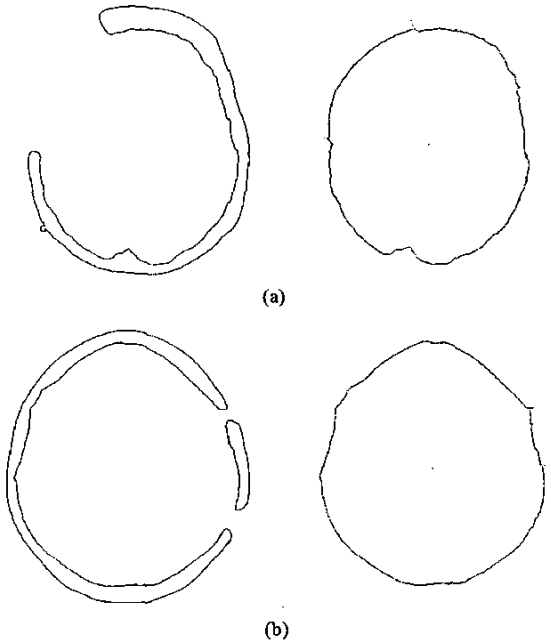

Fig. 9. Examples of two of the scenarios that the edge-following algorithm had to cope with and successfully negotiated. The left hand side illustrates the extracted edge data, and

the right hand side illustrates the final shape boundary: (a) a skull with a gap in the skull greater than 50 pixels, with no skull fragment; (b) a skull with a gap in the skull greater than 50 pixels, but where a skull fragment is present.

The edge-following algorithm failed on only one case, which is shown in Figure 10. In this case there is a surgical burr hole combined with an incomplete outer skull edge. The lower left outside edge of the skull is not completely in the active region of the image. In this example, the edge-following algorithm correctly negotiates the burr hole but fails when the outer edge goes outside the boundaries of the acquisition area.

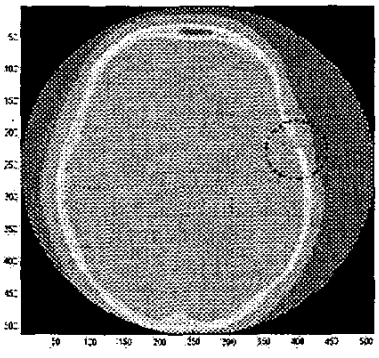

Fig. 10. The edge follower fails on this image. Once through the burr hole (circled), the edge follower correctly follows the outer edge until the skull meets the limit of the image, at the bottom left-hand corner. After this point, the edge follower wrongly follows the black semicircle, instead of the skull.

The current limitation of this algorithm is clearly its inability to process 10% of the database cases. In some cases, the incorrect axis of symmetry calculation is in fact due to the intrinsic asymmetry of the brain. The asymmetry may result in displacement of the centroid and hence an incorrect angle of rotation calculation.

5 Conclusions

The algorithm here described was found to operate successfully on the majority of cases, regardless of sex or focal abnormality. Its ineffectiveness on some 9.4% of cases will be henceforth investigated.

This study appears to be the first of its kind using CT data taken from large numbers of living patients. As stated in Duncan et al. [8]: "Our literature remains full of papers that evaluate algorithms on a few trial datasets from the home institution. This is sometimes in part due to simple lack of availability of a test set." We are fortunate enough to have a large and varied data set at our disposal, and this enables us to develop robust algorithms. The algorithm here described is written in Java, and is one of a suite of programs being used for data analysis of CT scans.

6 References

[1] I. Emelyanova, K. Parker, L. Cala, R. Linggard, Y. Attikiouzel, K. Michalak, N. Hicks, P. Robbins, F. Mastaglia, "Automatic Measurement of Brain Height from CT Scans", in *1st WSEAS (The World Scientific and Engineering Academy and Society) Transactions on Circuits*, vol. 1, pp. 165-168, 2002.

[2] G. N. Hounsfield, "Computerized axial tomography: estimation of spatial and density resolution capability", *The British Journal of Radiology*, vol. 46, pp. 1016-22, 1973.

[3] M. J. Atallah, "On Symmetry Detection", *IEEE Trans. Comput.*, vol. c-34, no. 7, pp. 663-666, 1985.

[4] G. Marola, "On the Detection of the Axes of Symmetry of Symmetric and Almost Symmetric Planar Images", *IEEE Trans. Pattern Analysis Mach. Intell.*, vol. 11, no. 1, pp. 104-198, 1989.

[5] J. Devenish, R. Linggard, K. Michalak, K. Parker, I. Emelyanova, L. Cala, Y. Attikiouzel, N. Hicks, P. Robbins, F. Mastaglia, *Quantifying Skull Shape*, {Accepted for presentation at the Seventh International Conference on Control, Automation, Robotic and Vision (ICARCV), 2-5 December, 2002, Singapore}, 2002.

[6] Y. Liu, R. T. Collins, W. E. Rothfus, "Robust Midsagittal Plane Extraction from Normal and Pathological 3-D Neuroradiology Images", *IEEE Trans. Med. Imag.*, vol. 20, no. 3, pp. 175-192, 2001.

[7] Y. Liu , R. T. Collins, W. E. Rothfus, "Automatic Extraction of the central Symmetry (Mid-Sagittal) Plane from Neuroradiology Images", Carnegie Mellon Univ., Pittsburgh, PA, The Robotics Institute, Tech. Rep. CMU-RI-TR-96-40, 1996.

[8] J. S. Duncan, N. A. Ayache, "Medical Image Analysis: Progress over Two Decades and the Challenges Ahead", *IEEE Trans. Pattern Analysis Mach. Intell.*, vol. 22, no. 1, pp. 85-105, 2000.

7 Acknowledgments

This research work was funded by a grant under the WA State Government Centres of Excellence Program—ARCME.